Physical Properties of Polyhedral Oligomeric Silsesquioxanes–Cycloolefin Copolymer Nanocomposites

Andrea Dorigato, Alessandro Pegoretti, Claudio Migliaresi

Dipartimento di Ingegneria dei Materiali e Tecnologie Industriali, Università di Trento, Via Mesiano 77-38100, Trento, Italy

Received 20 November 2008; accepted 10 April 2009
DOI 10.1002/app.30593
Published online 2 July 2009 in Wiley InterScience (www.interscience.wiley.com).

ABSTRACT: Properties of cycloolefin copolymer (COC)–polyhedral oligomeric silsesquioxanes (POSS) nanocomposites, prepared by melt compounding, have been investigated. Composites retained the optical transparency of the matrix up to a nanofiller content of 5 wt %. whereas for higher percentages the formation of a crystalline phase, due to the presence of agglomerated nanoparticles, was revealed by X-Ray diffraction (XRD). Differential scanning calorimetry (DSC) and thermogravimetric analysis (TGA) evidenced a significant decrease of the glass transition temperature (T_g) and of the thermal decomposition rate, with the POSS content. Similarly, at increasing filler content, both quasi-static tensile tests in the solid state and rheological measurements on melts showed a decrease of measured parameters (elastic modulus, ultimate elongation, loss and storage shear modulus, viscosity). These results were attributed to the formation of a soft interphase at the nanoparticles/polymer boundary due to the presence of isobutylic groups on POSS nanoparticles that limited the stress transfer process and acted in the COC matrix as a molecular lubricant agent. A small increase of the receding contact angle with the nanofiller content was also detected from dynamic contact angle (DCA) measurements. © 2009 Wiley Periodicals, Inc. J Appl Polym Sci 114: 2270–2279, 2009

Key words: nanocomposites; mechanical properties; rheology; thermal properties; transparency

INTRODUCTION

In the last decade, nanomaterials have attracted a lot of interest in the scientific and industrial field and the feeling that they could represent a big technological revolution for the next years is commonly diffused. There is a wide variety of nanomaterials available for various applications, for example in the automotive, in the biomedical, in the electronic, and in the information technology fields.

Polymer matrix nanocomposites were prepared for the first time by Toyota researchers, who produced a nylon 6-clay nanocomposite system for car cover belts.[1–3] Then several nanocomposite systems were developed, by using different polymeric matrices and nanofillers. Addition of a nanofiller to a polymeric matrix improves the mechanical behavior (stiffness,[4–7] failure properties,[6,8] and dimensional stability[9–11]), gas and solvents barrier properties,[12–14] thermal degradation, and chemical resistance.[4,14–16] Moreover, substantial improvements can be obtained by adding low filler content (not more than 5–10 wt %), avoiding the typical drawbacks (embrittlement, loss of transparency, loss of lightness) associated to the addition of traditional organic fillers.[17,18]

Among nanofillers available for the technological modification of polymeric materials, hybrid organic–inorganic fillers have gained a great importance in the last decade, because of their combination of an inorganic structure with organic functionalities.

Polyhedral oligomeric silsesquioxanes (POSS) were discovered and isolated for the first time in 1946,[19] starting from the hydrolytic condensation of trifunctional organosilicon monomers [for example $RSiCl_3$, $RSi(OMe)_3$. POSS are constituted by a Si—O cage, and by various organic functionalizations that can be chemically attached on silicon atoms of the cage. These organic moieties can be chemically or physically linked to the polymeric matrix.

Cycloolefin copolymers (COCs) are amorphous thermoplastics derived from the copolymerization of cycloolefin (often norbornene) and olefin monomers (ethylene or norbornene).[17,18,20–22] COCs possess high transparency, elevated glass transition and decomposition temperatures, low moisture absorption, good barrier, and mechanical properties. COCs are chemically resistant to hydrolysis, to acids, and to polar solvents such as ethanol and acetone.[23] Through their characteristic molecular structure and superior catalyst technology, COCs offer a wide range of properties variety, such as melt viscosity,

Correspondence to: A. Dorigato (andrea.dorigato@ing.unitn.it).

heat resistance, and deflection temperature that can be adjusted by varying the concentration of norbornenic groups. COC resins are suitable for the production of transparent moldings for use in optical data storage, lenses, sensors, products for the construction, and lighting sectors. These copolymers are also of particular interest for primary packaging of pharmaceuticals, medical devices, and diagnostic disposables. New applications have been recently developed for blends of COC, with a variety of polyolefins, and some articles can be found in literature on this topic. For example, Pegoretti et al.[21] prepared polypropylene (PP)/COC blends, to study the effects of the fibrous phase structure on tensile mechanical properties, whereas Kolarik et al.[20] studied nonlinear tensile creep behavior of high-density polyethylene/COC blends.

To our knowledge, only a few works dealing with the preparation and characterization of COC-based nanocomposites have been published. For example, Ou and Hsu[17,18] prepared a series of organic COC-silica nanocomposites by solution blending, finding an enhancement of the glass transition temperature and of the decomposition temperature with the silica content, without affecting the intrinsic transparency of the matrix. COC/clay nanocomposites prepared by Wu and Wu[22] through a solution mixing process showed significant improvements in the storage modulus and water permeability with respect to the neat COC matrix.

In a recent article, COC/POSS nanocomposites were characterized for the first time by Iyer et al.[24] Although the optical clarity was generally retained, mechanical properties were negatively affected by the introduction of POSS in the matrix.

Starting from the considerations reported in that article, we have investigated the properties of COC–POSS nanocomposites by using different amounts of POSS nanoparticles, to detect their influence on the final material properties, with particular attention to their mechanical and thermal behavior. The effect of POSS nanoparticles on the optical behavior and on the surface properties of COC was also evaluated.

EXPERIMENTAL PART

Materials

An allylisobutyl POSS (OL1118), supplied by Hybrid Plastics® (USA) was used as nanofiller (chemical formula $C_{31}H_{68}O_{12}Si_8$, molecular weight 857.55 $g \cdot mol^{-1}$). As it can be seen in Figure 1, this nanohybrid is constituted by a siliceous core surrounded by seven isobutylic groups, whereas the organic moiety is represented by an allylic group. This POSS grade was chosen because the presence of hydrocarbon end groups around the SiO_2 cage should favor the chemical compatibility with the polyolefinic COC matrix.

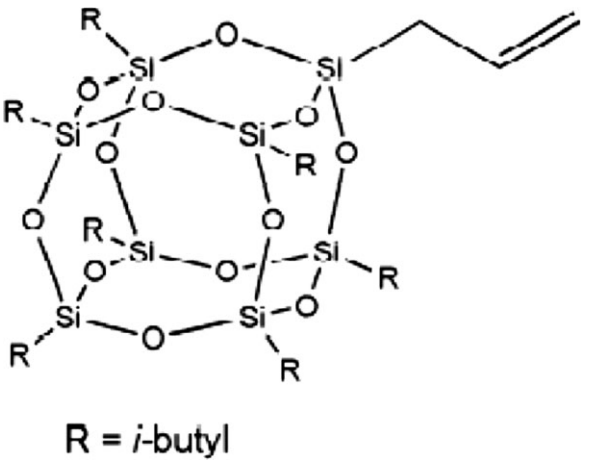

Figure 1 Chemical structure of Hybrid Plastics® allylisobutyl POSS.

The polymeric matrix was an amorphous COC, trade name Topas® 8007, supplied by Ticona (Germany), consisting of 30% bicyclo[2.2.1]hept-2-ene (norbornene) units and 70% ethylene units (MFI = 34.3 g · 10 min^{-1} at 230°C and 5 kg, density = 1.014 $g \cdot cm^{-3}$, T_g = 81°C). All materials were used as received.

Preparation of samples

Melt mixing was performed in a PolyLab Rheomix R600 internal mixer (Thermo Haake® GmbH, Germany) equipped with roller rotors and a torque rheometer. COC (about 50 g) and various amounts of POSS nanofillers (0, 1, 5, and 10 wt %) were loaded in the chamber of the internal mixer and compounded at a temperature of 190°C at a rotors speed of 90 rpm. The mixing time was kept equal to 15 min for all the samples. The resulting compound was compression molded in a laboratory press (Carver Inc.®, IN) at a temperature of 190°C and at a pressure of 0.2 kPa, to produce square sheets 200 mm wide and 0.6 mm thick. The specimens required for the various characterization techniques have been machined from the sheets.

In this article, the pure matrix samples have been denoted as COC, whereas nanocomposites have been identified as POSS followed by the filler weight percentage (for example POSS5 indicates a COC nanocomposite with 5 wt % of POSS).

Experimental activities

FTIR tests were conducted by using a Perkin Elmer Spectrum One FTIR-ATR analyser in a scanning interval between 600 and 1800 cm^{-1}.

For X-ray diffraction (XRD) analyses a Philips Xpert HRD diffractometer was used, by using Cu Kα (λ = 0.15406 nm) radiation, generated at a voltage of 40 kV and with a current of 30 mA. The diffraction angle 2θ was scanned from 1° to 30° at a step increment Δθ of $1°\cdot min^{-1}$.

A Mettler DSC30 differential scanning calorimeter was used for calorimetric tests, performed in a temperature range between 0°C and 200°C at a heating rate = $10°C\cdot min^{-1}$, under a nitrogen flow of 100 $mL\cdot min^{-1}$.

Rheological measurements were performed with a TA Instrument Ares Rheometer in dynamic mode. Plates with a diameter of 25 mm were selected and a plate-to-plate gap of 0.5 mm was adopted. All samples were tested at a temperature of 190°C in a frequency range from 0.05 $rad\cdot s^{-1}$ to 200 $rad\cdot s^{-1}$, at a constant shear strain of 1%. Six points per decade were collected.

Dynamic mechanical thermal analysis was performed with a Polymer Laboratories MKII testing machine on rectangular samples 15 mm long, 5 mm wide, and 0.6 mm thick applying a sinusoidal strain with a frequency of 1 Hz and an amplitude of 64 μm. A heating rate of $3°C\cdot min^{-1}$, from 20°C to 100°C, was selected for all tests.

Quasi-static mechanical tensile properties were determined by using an Instron 4502 tensile testing machine, equipped with a 1 kN load cell on ISO 527 type 1BA dog-bone specimens (gage length 30 mm, distance between grips 55 mm, crosshead speed of 1 $mm\cdot min^{-1}$). The strain was recorded by using a clip-gage extensometer (Instron model 2620-601, gage length 12.5 mm).

Thermogravimetric analysis (TGA) was performed through a Mettler TG50 thermobalance, from 30°C to 700°C at a heating rate of $10°C\cdot min^{-1}$ under a nitrogen flow of 100 $mL\cdot min^{-1}$. Mass loss and mass loss rate were recorded for every sample.

Surface properties of pure COC and relative nanocomposites were evaluated through dynamic contact angle measurements, by using a Cahn DCA-322 dynamic contact angle analyzer. Rectangular samples 10 mm wide and 0.6 mm thick were dipped in water at room temperature (surface tension σ = 72.7 $mJ\cdot m^{-2}$) for 8 mm with a dipping speed of 20 $\mu m\cdot s^{-1}$ and then extracted at the same speed. At least three tests were conducted for each sample. In this way, dynamic advancing and receding contact angles were evaluated by using the Willhelmy equation:

$$\cos\,\theta = \frac{F}{L\,\sigma} \tag{1}$$

where F is the measured force during the dipping, L is the wetted perimeter, σ is the surface tension of the liquid.

Digital pictures for the evaluation of the optical transparency were acquired by a Nikon Coolpix 4500 digital camera at a distance of 30 cm from the specimens (thickness = 0.6 mm). To evaluate the optical transparency of the nanocomposites, near UV–visible light spectroscopic analyses were performed, by using a Jasco V-570 spectrofotometer, in a wavelength range of 200–850 nm.

RESULTS AND DISCUSSIONS

FTIR spectra of COC and relative nanocomposites are reported in Figure 2. Filled samples present an absorption peak at about 1100 cm^{-1}, whose intensity is proportional to the POSS content. This absorbance peak can be attributed to Si—O—Si stretching vibrations, indicating the presence of POSS on the surface, as confirmed by other literature articles on POSS nanocomposites.[25–30]

X-ray diffractograms of COC matrix, POSS powder, and relative nanocomposites are reported in Figure 3. The amorphous COC matrix present a broad diffraction peak at 2θ = 17.5°, whereas the very narrow diffraction peak at 2θ = 8° of POSS powder clearly confirms its crystalline structure. The absence of this latter peak in the POSS1 and POSS5 nanocomposites and its presence in the POSS10 samples reveals that nanoparticles were well dispersed in the lower filler content materials, whereas agglomeration occurred in the higher filler content sample. The presence of a distinct diffraction peak for POSS nanofillers is well documented in literature, especially for methyl-POSS nanopowders, in particular the destruction of the crystalline order due to the nanoparticles disagglomeration was well described by Fina et al.[25] and Chen and Chiou[31] in their work on PP–POSS nanocomposite systems.

DSC curves of COC and relative nanocomposites are presented in Figure 4, whereas the most important results obtained from first and second DSC scans are summarized in Table I. The melting peak at about 40°C for the pure POSS powder indicates the presence of a crystalline phase in the material with a melting enthalpy of 13 $J\cdot g^{-1}$. A small signal, with specific enthalpy of 4.6 $J\cdot g^{-1}$, can be detected in the POSS10 sample, indicating the presence of agglomerated POSS nanoparticles with a crystalline order in these composites. On the other hand, the absence of melting peaks in the nanocomposites with lower loading levels is an evidence that POSS nanoparticles are completely disaggregated and well dispersed in the amorphous COC matrix. These data are consistent with the XRD results previously presented. The presence of a solubility limit for POSS in polycarbonate (PC) and phenoxy resins was well described by Iyer and Schiraldi,[32] who found the presence of POSS aggregates for filler content higher

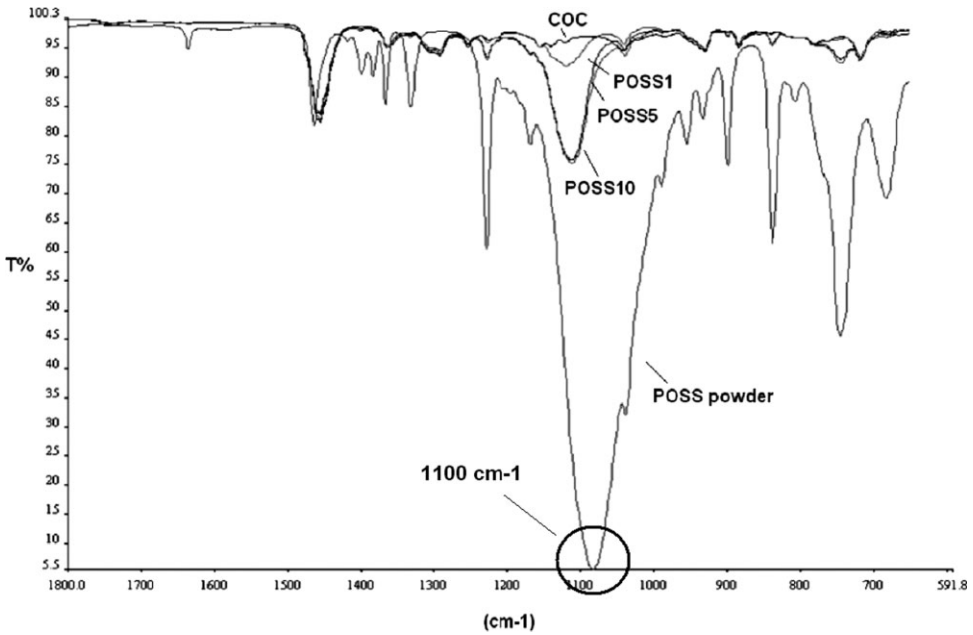

Figure 2 FTIR spectra of COC, POSS powder, and relative nanocomposites.

than 5 wt %. Furthermore, the importance of polymer-filler interactions in the miscibility of POSS fillers was underlined by Zhou et al.[33,34] who obtained good particles dispersion for reactive blended PP/POSS composites.

The glass transition temperature of the COC matrix decreases with the POSS content, from 81°C for the unfilled material to 71°C for POSS10 sample. As already reported by Kim et al.[35] for PET–POSS nanocomposites and by Pracella et al.[36] for PP-POSS nanocomposites, also in the present case the incorporation of small amounts of POSS acts as an inert molecular diluent, reducing the T_g of the matrix.

Dynamic shear moduli (G' and G'') of pure COC and relative nanocomposites are shown in Figure 5(a,b), respectively, whereas loss factors and viscosity values are represented in Figure 5(c,d). It is evident that the presence of POSS nanoparticles in the material leads to a slight decrease of both the storage and the loss shear modulus, whereas tanδ is slightly enhanced by the nanofiller addition. Furthermore, the viscosity of the filled samples is lower than that of the pure COC, especially for highly filled samples, thus confirming the role played by POSS nanoparticles as molecular lubricant agents in the polymeric matrix. These results are in contrast

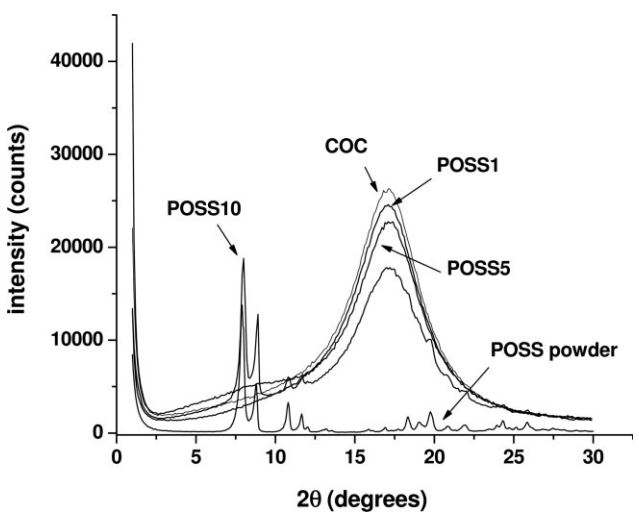

Figure 3 XRD diffractograms of COC matrix, POSS powder, and relative nanocomposites.

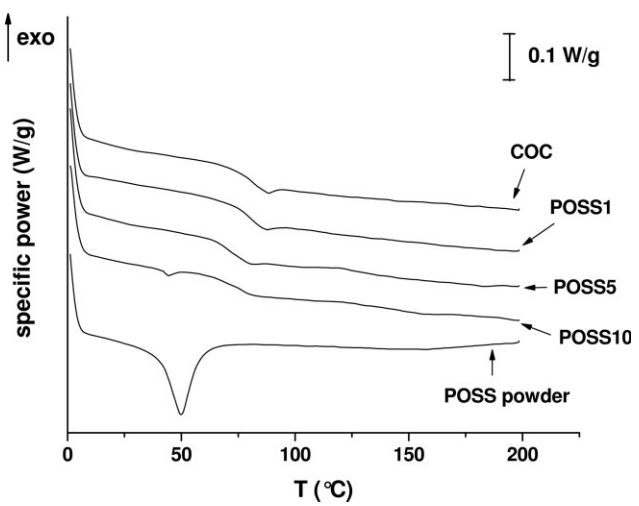

Figure 4 DSC curves of COC and relative nanocomposites (first scan).

TABLE I
DSC Data for COC Matrix, Poss Powder, and Relative Nanocomposites

Sample	T_{g1} (°C)	T_{g2} (°C)	ΔHm_1 (J·g^{-1})	ΔHm_2 (J·g^{-1})	T_{m1} (°C)	T_{m2} (°C)
COC	80.8	78.9	–	–	–	–
POSS1	80	78.1	–	–	–	–
POSS5	69.8	74.9	–	–	–	–
POSS10	71.3	75.3	4.6	7.1	43.8	41.6
POSS powder	–	–	13.04	15.18	49.2	41.6

T_{g1}: glass transition temperature—first scan.
T_{g2}: glass transition temperature—second scan.
ΔHm_1: specific heat of fusion—first scan.
ΔHm_2: specific heat of fusion—second scan.
T_{m1}: melting temperature—first scan.
T_{m2}: melting temperature—second scan.

with the increase of glass transition temperature and of viscosity generally reported for polymeric nanocomposite systems, as summarized by Cassagnau[37] in an article on the rheological properties of silica and clay filled composites, and by Kim et al.[35] who found a slight enhancement of the viscosity of PET–

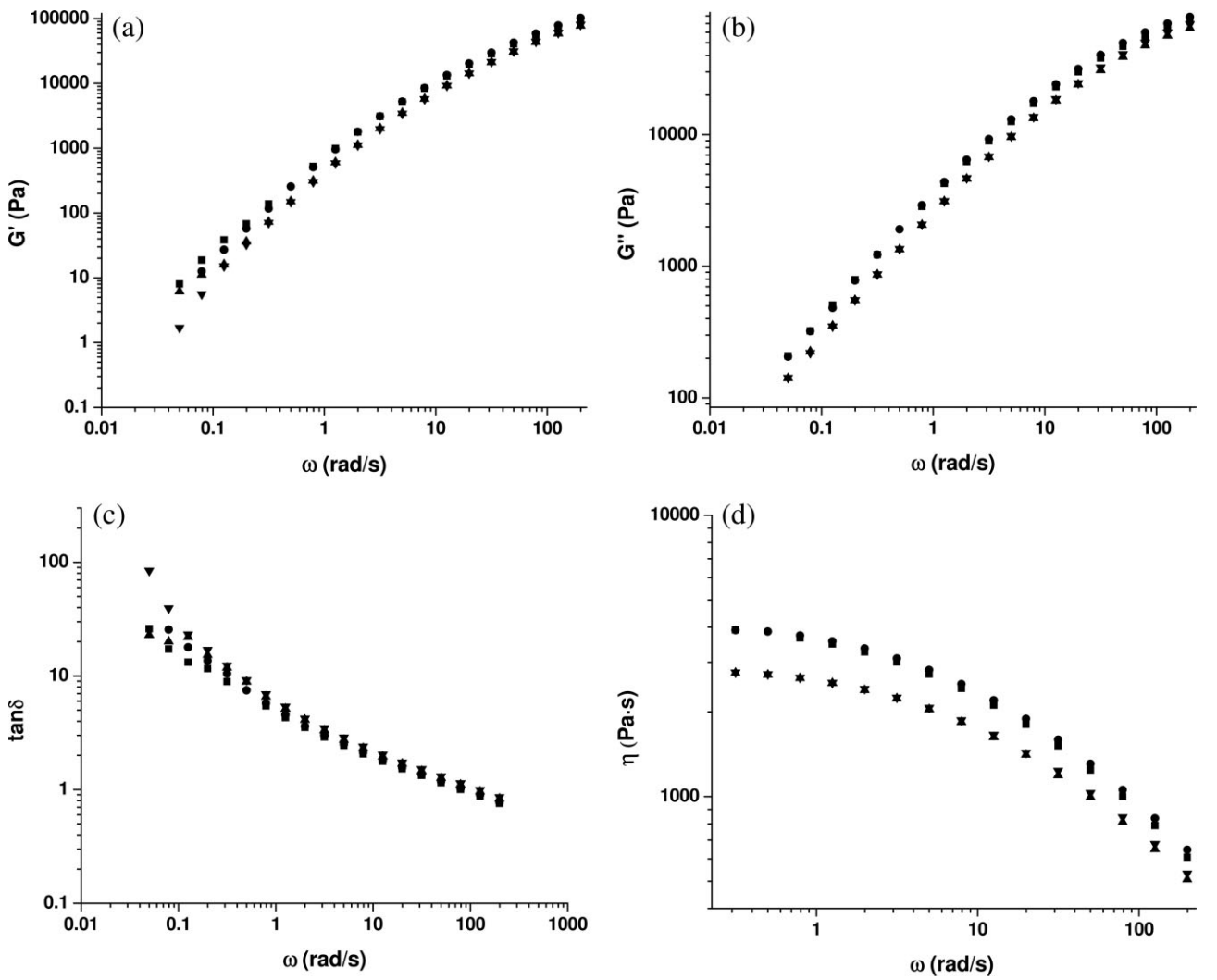

Figure 5 (a) Storage shear modulus (G') of COC and relative nanocomposites from dynamic rheological tests. (■) COC, (●) POSS1, (▲) POSS5, (▼) POSS10. (b) Loss shear modulus (G'') of COC and relative nanocomposites from dynamic rheological tests. (■) COC, (●) POSS1, (▲) POSS5, (▼) POSS10. (c) Tanδ values of COC and relative nanocomposites from dynamic rheological tests. (■) COC, (●) POSS1, (▲) POSS5, (▼) POSS10. (d) Viscosity values (η) of COC and relative nanocomposites from dynamic rheological tests. (■) COC, (●) POSS1, (▲) POSS5, (▼) POSS10.

POSS nanocomposites with respect to the unfilled matrix. Furthermore, Zhou et al.[38] studied dynamic rheological properties of epoxycyclohexyl-POSS PET systems, finding an increase of the shear viscosity with the filler content, associated to the disappearance of the Newtonian plateau for highly filled samples. The effect of POSS nanofillers on rheological properties of the samples is dependent on the polymer-filler interaction, as reported by Zhou et al.[39] in their work on PP–POSS nanocomposites. Physically blended composites showed a slight decrease of G', G'', and shear viscosity values for lower filler contents (<2 wt %), whereas for higher POSS loadings rheological properties started to increase. On the contrary, reactive blended composites presented a constant increase of the viscosity with the filler content, associated to a solid-like behavior for highly filled samples.

Figure 6(a,b) summarize tensile storage modulus, E', and damping, tanδ, thermograms for COC and relative nanocomposites, as obtained from DMTA tests. The shift to lower temperatures of the E' curves and of the tanδ maxima, confirms the decrease of the glass transition temperatures in nanocomposites, in accordance with the experimental evidences of DSC tests. Moreover, the room temperature storage modulus for the filled samples is slightly lower than that of the pure COC. A similar trend was already observed by Zhao and Schiraldi[40] on PC–POSS nanocomposite systems: even in that work the reduction of the glass transition temperature and of the storage modulus were attributed to the plasticization effect of POSS nanoparticles. Furthermore, Iyer and Schiraldi[32] analyzed dynamic properties of POSS filled PC and phenoxy resin (PKFE) composites. Although the incorporation of trisilanol-POSS in PKFE led to a considerable increase of the storage modulus with the filler content and to a slight increase of the glass transition temperature, for PC-POSS composites both storage modulus and T_g showed a substantial decrease. It was concluded that an improvement of the mechanical properties is possible only when strong physical interactions develop in the composite. The importance of polymer-filler interactions was confirmed by Zhou et al.,[34] who recently studied dynamic mechanical properties of PP–POSS systems prepared by physical blending and by reactive blending process. E' of physically blended composites decreased at increasing POSS content in the polymer glassy state, probably because POSS induced in the PP the formation of less stiff β-crystalline regions. On the contrary, the moduli of all the reactively blended composites were higher, due to the hindering effect exerted by POSS on the PP chain mobility.

Representative curves of quasi-static tensile tests of COC and relative nanocomposites are represented in Figure 7, whereas elastic moduli and tensile properties at break are summarized in Table II. It is evident that the elastic modulus and the stress at break decrease as the POSS concentration increases, especially for the 10 wt % filled sample, whereas the strain at break was practically insensitive to the nanofiller addition. The addition of a rigid nanofiller usually increases stiffness, melt viscosity, and glass transition temperature of a polymer.[7,9,10,18,41–49] However, the detrimental effect of POSS introduction on the mechanical properties of polymeric matrices has already been reported in the literature. Baldi et al.[50] ascribed the drop of the mechanical properties of PP/POSS nanocomposites to the formation of a soft interphase caused by the presence of hydrocarbons functionalizing the POSS cage. The organic functionalization moieties of the POSS filler used in this work were hydrocarbon chains of four

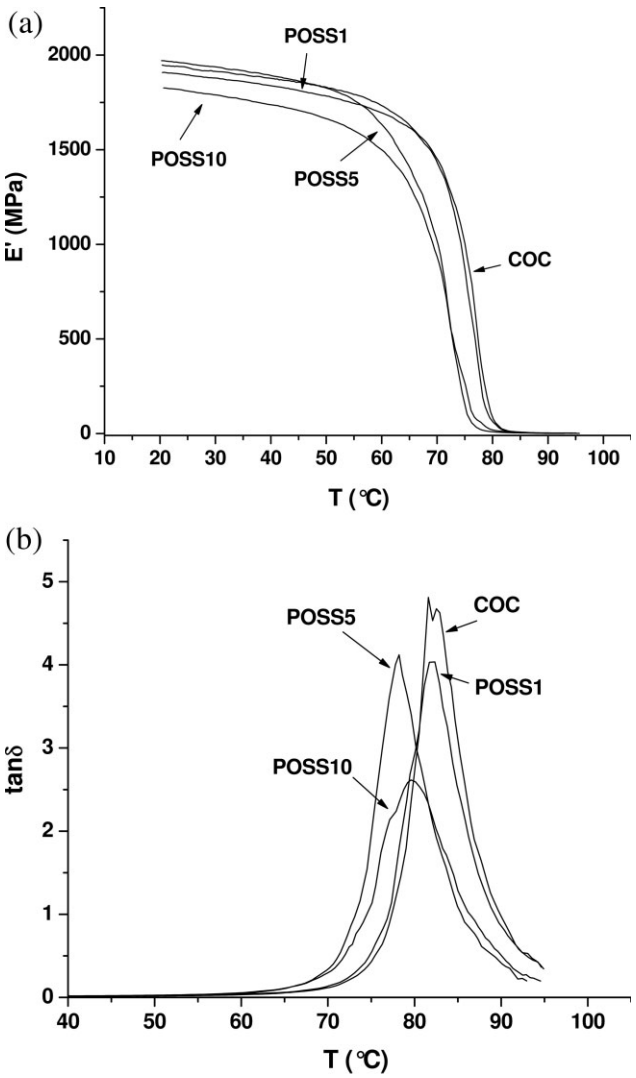

Figure 6 (a) Storage modulus values for COC and relative nanocomposites from DMTA tests. (b) Tanδ values of COC and relative nanocomposites from DMTA tests.

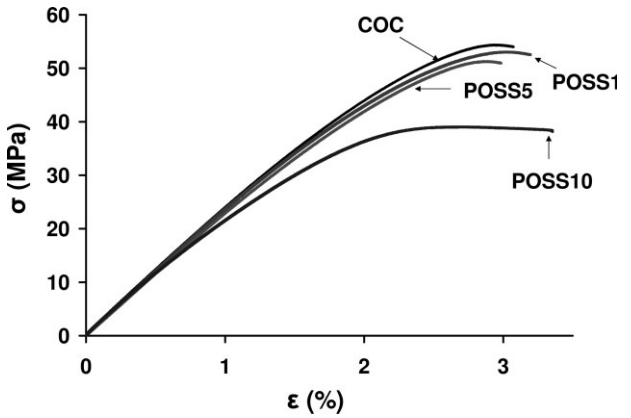

Figure 7 Representative curves from quasi-static tensile tests of COC, and relative nanocomposites.

(allylisobutyl-POSS) carbon atoms. Thus, these POSS molecules can be considered as particles having a siliceous hard-core enveloped by a hydrocarbon soft shell. In composites, where a polymer matrix embeds particles having a hard core surrounded by a soft shell, the stress transfer from the matrix to the core can be considerably impaired and the reinforcing action could be even nullified. For example, Ricco' et al.[51] demonstrated by means of a micromechanical model that the stiff core does not share the load if the thickness of the shell is higher than about 25% of the radius of the hard core. This means that POSS aggregates behave as soft, rubber-like particles, unable to supply mechanical reinforcement, so inducing a stiffness reduction.

Thermogravimetric curves of COC and relative nanocomposites are reported in Figure 8(a), whereas derivative of the mass loss is represented in Figure 8(b). In Table III, the main results from TGA tests are summarized. It is evident that the onset of the degradation process for POSS1 sample is slightly higher than that of pure COC matrix, whereas for nanocomposites at higher filler amount $T_{2\%}$ values are markedly decreasing. This result can be explained considering that this nanohybrid is composed by a hard inorganic core surrounded by a soft hydrocarbon shell that accounts for 50% of the entire nanoparticle weight. The degradation resistance of the organic shell, containing mainly isobutylic groups, is lower than that of the polymeric chain of

TABLE II
Quasi-Static Tensile Mechanical Properties of COC and Relative Nanocomposites

Sample	E (GPa)	σ_r (MPa)	ε_r (%)
COC	2.41 ± 0.06	54.1 ± 0.2	3.04 ± 0.2
POSS1	2.39 ± 0.05	52.4 ± 0.4	3.12 ± 0.1
POSS5	2.33 ± 0.06	51.0 ± 0.6	2.97 ± 0.1
POSS10	2.31 ± 0.13	39.3 ± 0.4	3.51 ± 0.5

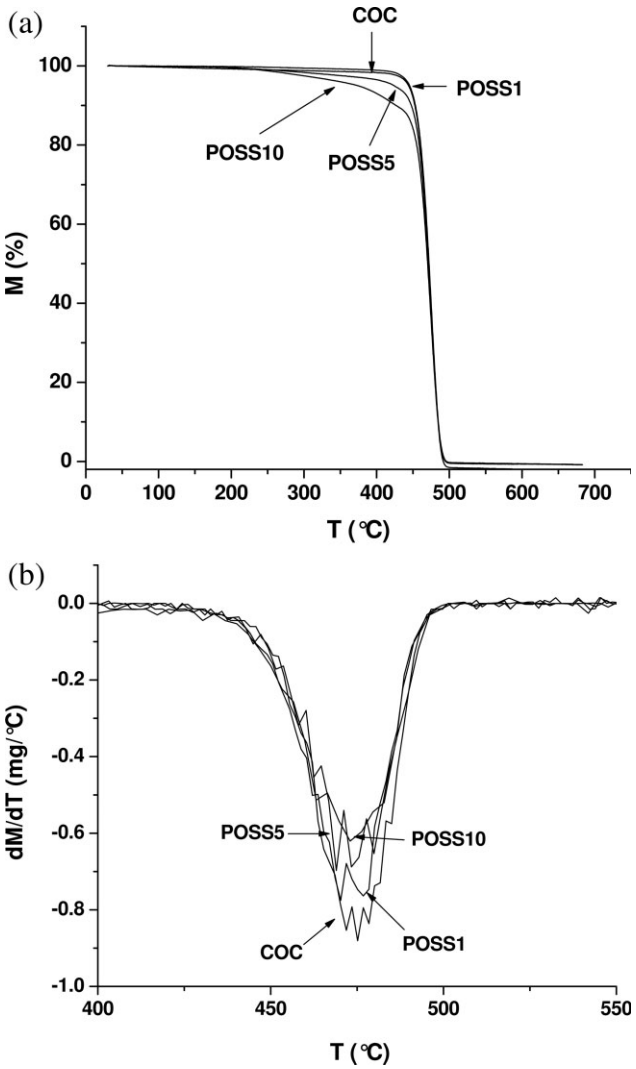

Figure 8 (a) Thermogravimetric curves of POSS powder, COC, and relative nanocomposites. (b) Derivative of the mass loss from TGA tests of POSS powder, COC, and relative nanocomposites.

COC, very long and stiffened by the presence of norbonenic groups. It is important to underline that the maximum mass loss rate for pure COC was bigger than that of POSS10 sample. The reduction of the peak decomposition rate can be explained considering that the organic–inorganic component of Si and O in the cage-like framework can decrease the

TABLE III
TGA Data for COC and Relative Nanocomposites

Sample	$T_{2\%}$[a] (°C)	MMLR[b] (mg/°C)
COC	419.0	0.88
POSS1	429.3	0.77
POSS5	322.7	0.70
POSS10	280.3	0.62

[a] $T_{2\%}$: temperature corresponding to 2 wt % mass loss.
[b] MMLR: maximum mass loss rate.

TABLE IV
Advancing and Receding Contact Angles of COC and Relative Nanocomposites Evaluated by Dynamic Contact Angle Measurements

Sample	ADV (°)	REC (°)
COC	101.6 ± 1.8	53.7 ± 0.3
POSS1	103.1 ± 4.1	53.2 ± 3.8
POSS5	99.3 ± 0.4	55.2 ± 1.7
POSS10	102.9 ± 1.7	62.9 ± 1.6

thermal conductivity of the matrix, preventing heat from fast spreading. Moreover, isobutylic moieties could promote secondary reactions during polymer degradation, leading to partial matrix charring, instead of complete volatilization. A similar trend in the degradation rate for POSS filled samples was already reported by Fina et al.[25] in a work on PP/POSS nanocomposites and by Liu et al.[52] in an article on PS–POSS systems. Even in this case polymer-filler interaction is fundamental to interpret thermal stability of POSS filled composite. Zhou et al.[53] found that physically blended POSS–PP nanocomposites showed a decrease of decomposition temperatures with increasing filler content, due to the poor thermal stability of the POSS powder. On the contrary, reactive blended composites displayed higher decomposition temperatures, due to the increased thermal stability of the grafted POSS. In any case, flame retardant properties, studied with a cone calorimeter, were significantly improved for both physically and reactively blended composites.

The surface properties of these materials, with the determination of the advancing and the receding contact angles of COC and relative nanocomposite, evaluated by dynamic contact angle measurements, are summarized in Table IV. Although the advancing contact angle is not influenced by the presence of POSS nanoparticles, the receding contact angle slightly increases with the POSS content, from 54° of pure POSS to 63° of POSS10 sample. The enhancement of the surface hydrophobicity due to the presence of POSS nanofillers is well documented in literature, for example in the work of Misra et al.[26] on PP–POSS nanocomposites. The increase in the water contact angle is due to the hydrophobic nature of the nanocomposite surface. This can be explained by the low surface energy of COC matrix itself and by the cumulative effect of the isobutyl groups attached to the corner silicon atoms of the POSS cage. Low surface energy of POSS nanoparticles and their nanometric size causes them to preferentially migrate toward the surface and produces a gradient in POSS distribution from bulk to the surface. The hydrophobic functionalities of POSS nanoparticles, to reduce the free surface energy, could migrate and substitute the hydrophilic domains on the polymer surface. In a polymeric system, advancing contact angle is more sensitive to the low surface energy domains, whereas receding contact angle is more sensitive to the high surface energy domains. Because of the hydrophobic nature of COC, the surface of pure COC was almost completely saturated by hydrophobic domains and the effect of hydrocarbon functionalities of POSS was negligible for the dynamic advancing angle, while the receding contact angle, being more sensitive to hydrophilic domains, could be partially altered by the presence of POSS nanoparticles.

Photographs for the evaluation of the transparency of the samples are reported in Figure 9. For the pure COC, POSS1, and POSS5 samples, the transparency is very high in the visible light range, whereas the transmittance had a very sharp drop in the near UV region. This optical behavior is typical for transparent amorphous polymeric matrices, as reported in the articles of Ou and Hsu[17,18] on COC-silica nanocomposite systems. It is evident that the transparency of the material was maintained up to a loading level of 5 wt % confirming the good dispersion degree of POSS nanoparticles already suggested by the absence of the POSS melting peak in DSC tests. Furthermore, POSS10 sample is partially hazy, because of the partial agglomeration of the nanoparticles, and the partial preservation of the crystalline order of POSS nanoparticles. To support the experimental evidences of the photographs, UV–visible light spectroscopy results are reported in Figure 10.

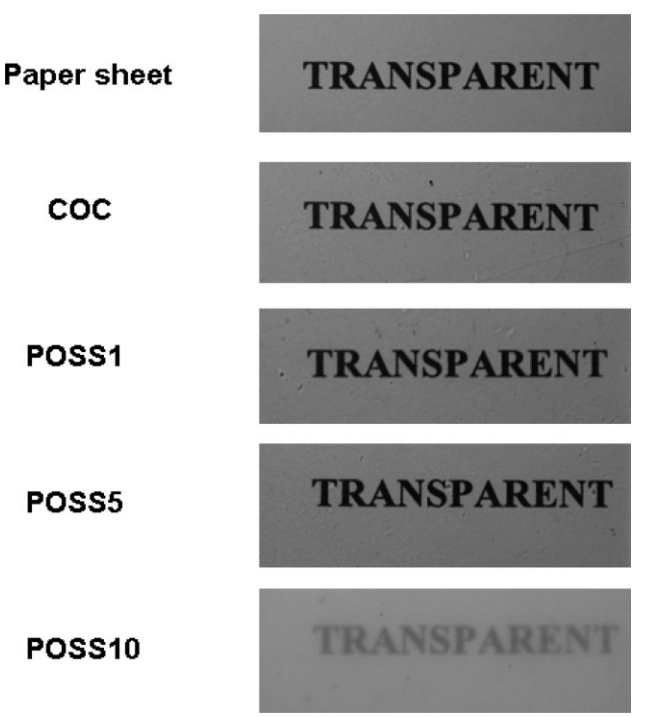

Figure 9 Evaluation of the transparency of the samples of COC and relative nanocomposites.

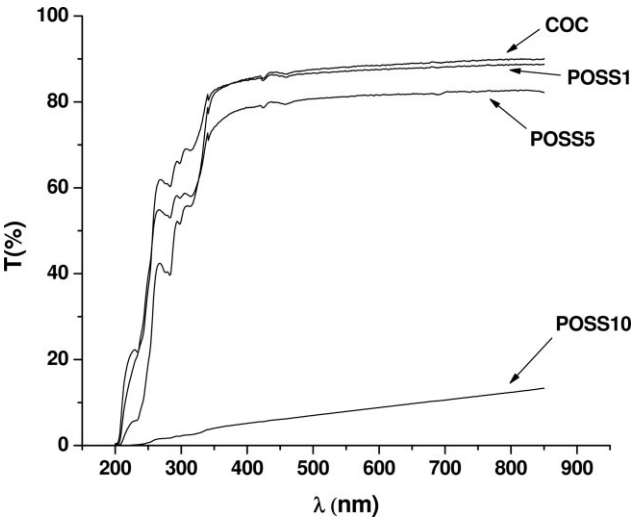

Figure 10 UV–visible light spectroscopy of COC and relative nanocomposites.

It is evident that transmittance values for POSS1 sample are very similar to those of the unfilled matrix (near 90% in the visible light range), and the transparency is substantially maintained also for POSS5 sample (about 83%). Because of the presence of agglomerated crystalline domains, POSS10 is completely hazy, consequently transmittance values were below 15% in the entire wavelength range. The retention of transparency for POSS filled composites was already evidenced by Iyer et al.,[24] who studied four different amorphous materials-based nanocomposites. Even if a high optical clarity could be substantially retained for most samples, the presence of strong particle-matrix interactions was considered to play a key role in preserving the optical clarity of the matrix while enhancing their tensile mechanical properties.

CONCLUSIONS

COC–POSS nanocomposites were prepared to determine the influence of this nanofiller on the thermomechanical properties of the material. Rheological tests showed a plasticizing effect of the POSS nanoparticles consisting in a decrease of the dynamic shear moduli and of the viscosity of the system with the POSS concentration. Concurrently, a drop in the COC glass transition temperature due to the presence of POSS nanoparticles was revealed by both DSC and DMTA tests. Furthermore, quasi-static tensile tests evidenced a decrease of the elastic modulus and POSS nanopowders due to a plasticization effect, probably due to the presence of a soft interphase, limiting the stress transfer process, and acting as a molecular lubricant agent.

DSC tests also revealed the presence of a crystalline phase for the 10 wt % filled sample, due to nanoparticles agglomeration, confirmed by XRD analysis. In fact, this sample was partially hazy, while at lower POSS concentrations COC retained most of its original transparency.

TGA tests revealed the efficacy of these nanofillers in reducing the mass loss rate during the thermal degradation process. Dynamic contact angle measurements confirmed the surface hydrophobic effect of these nanohybrids, especially on the receding component and for the highest filler content.

References

1. Kojima, Y.; Usuki, A.; Kawasumi, M.; Okada, A.; Kurauchi, T.; Kamigaito, O. J Polym Sci: Polym Chem 1993, 31, 983.
2. Kojima, Y.; Usuki, A.; Kawasumi, M.; Okada, A.; Kurauchi, T.; Kamigaito, O.; Kaji, K. J Polym Sci: Polym Phys 1994, 32, 625.
3. Kojima, Y.; Usuki, A.; Kawasumi, M.; Okada, A.; Kurauchi, T.; Kamigaito, O.; Kaji, K. J Polym Sci: Polym Phys 1995, 33, 1039.
4. Mandalia, T.; Bargaya, F. J Phys Chem Solids 2005, 67, 836.
5. Yuan, Q.; Misra, R. D. K. Polymer 2006, 47, 4421.
6. Zhang, J.; Jiang, D. D.; Wilkie, C. A. Thermochim Acta 2005, 430, 107.
7. Zhang, Z.; Yang, J. L.; Friedrich, K. Polymer 2004, 45, 3481.
8. Zhang, M. Q.; Rong, M. Z.; Zhang, H. B.; Friedrich, K. Polym Eng Sci 2003, 43, 490.
9. Bondioli, F.; Dorigato, A.; Fabbri, P.; Messori, M.; Pegoretti, A. Polym Eng Sci 2008, 48, 448.
10. Pegoretti, A.; Dorigato, A.; Penati, A. Express Polym Lett 2007, 1, 123.
11. Starkova, O.; Yang, J. L.; Zhang, Z. Compos Sci Technol 2007, 67, 2691.
12. Choi, W. J.; Kim, S. H.; Kim, Y. J.; Kim, S. C. Polymer 2004, 45, 6045.
13. Gorrasi, M.; Tortora, M.; Vittoria, G. J Polym Sci B: Polym Phys 2005, 43, 2454.
14. Tortora, M.; Gorrasi, M.; Vittoria, G.; Galli, V.; Ritrovati, S.; Chiellini, E. Polymer 2002, 43, 6147.
15. Zhang, M.; Sundararaj, U. Macromol Mater Eng 2006, 291, 697.
16. Zhao, C.; Qin, H.; Gong, F.; Feng, M.; Zhang, S.; Yang, M. Polym Degrad Stab 2005, 87, 183.
17. Ou, C. F.; Hsu, M. C. J Appl Polym Sci 2007, 104, 2542.
18. Ou, C. F.; Hsu, M. C. J Polym Res 2007, 14, 373.
19. Scott, D. W. J Am Chem Soc 1946, 68, 356.
20. Kolarik, J.; Pegoretti, A.; Fambri, L.; Penati, A. Polym Eng Sci 2006, 47, 1363.
21. Pegoretti, A.; Kolarik, J.; Fambri, L.; Penati, A. Polymer 2003, 44, 3381.
22. Wu, T. M.; Wu, C. W. J Polym Sci, Part B: Polym Phys 2005, 43, 2745.
23. Phillips, S. H.; Haddad, T. S.; Tomczak, S. J. Curr Opin Solid State Mater Sci 2004, 8, 21.
24. Iyer, S.; Abu-Ali, A.; Detwiler, A.; Schiraldi, D. A. ACS Symp Ser 2007, 964, 313.
25. Fina, A.; Tabuani, D.; Frache, A.; Camino, G. Polymer 2005, 46, 7855.
26. Misra, R.; Fu, B.; Morgan, S. E. J Polym Sci, Part B: Polym Phys 2007, 45, 2441.
27. Ramasundaram, S. P.; Kim, K. J. Macromol Symp 2007, 249, 295.
28. Wang, Y. Z.; Chen, W. Y.; Yang, C. C.; Lin, C. L.; Chang, F. C. J Polym Sci, Part B: Polym Phys 2007, 45, 502.
29. Xiao, F.; Sun, Y.; Xiu, Y.; Wong, C. P. J Appl Polym Sci 2007, 104, 2113.
30. Xu, H.; Yang, B.; Wang, J.; Guang, H.; Li, C. J Polym Sci, Part A: Polym Chem 2007, 45, 5308.

31. Chen, J. H.; Chiou, Y. D. J Polym Sci, Part B: Polym Phys 2006, 44, 2122.
32. Iyer, S.; Schiraldi, D. A. Macromolecules 2007, 40, 4942.
33. Zhou, Z.; Cui, L.; Zhang, Y.; Zhang, Y.; Yin, N. J Polym Sci Part B: Polym Phys 2008, 46, 1762.
34. Zhou, Z.; Cui, L.; Zhang, Y.; Zhang, Y.; Yin, N. Eur Polym J 2008, 44, 3057.
35. Kim, J. K.; Yoon, K. H. Y.; Bang, D. S. B.; Park, Y. B. P.; Kim, H. U. K.; Bang, Y. H. B. J Appl Polym Sci 2008, 107, 272.
36. Pracella, M.; Chionna, D.; Fina, A.; Tabuani, D.; Frache, A.; Camino, G. Macromol Symp 2006, 234, 59.
37. Cassagnau, P. Polymer 2008, 49, 2183.
38. Zhou, Z.; Yin, N.; Zhang, Y.; Zhang, Y. J Appl Polym Sci 2008, 107, 825.
39. Zhou, Z.; Zhang, Y.; Zhang, Y.; Yin, N. J Polym Sci Part B: Polym Phys 2008, 46, 526.
40. Zhao, Y.; Schiraldi, D. A. Polymer 2005, 46, 11640.
41. Gopakumar, T. G.; Lee, J. A.; Kontopoulou, M.; Parent, J. S. Polymer 2002, 43, 5483.
42. Hotta, S.; Paul, D. R. Polymer 2004, 45, 7639.
43. Kato, M.; Okamoto, H.; Hasegawa, N.; Tsukigase, A.; Usuki, A. Polym Eng Sci 2003, 43, 1312.
44. Kontou, E.; Niaounakis, M. Polymer 2006, 47, 1267.
45. Lee, J. H.; Jung, D.; Hong, C. E.; Rhee, K. Y.; Advani, S. G. Compos Sci Technol 2005, 65, 1996.
46. Ranade, A.; Nayak, K.; Fairbrother, D.; D'souza, N. A. Polymer 2005, 46, 7323.
47. Wang, K. H.; Choi, M. H.; Koo, C. M.; Xu, M.; Chung, I. J. J Polym Sci, Part B: Polym Phys 2002, 40, 1454.
48. Wanjale, S. D.; Jog, J. P. Polym Int 2004, 53, 101.
49. Zhang, J.; Jiang, D. D.; A, W. C. Polym Degrad Stab 2006, 91, 298.
50. Baldi, F.; Bignotti, F.; Fina, A.; Tabuani, D.; Ricco', T. J Appl Polym Sci 2007, 105, 935.
51. Ricco', T.; Pavan, A.; Danusso, F. Polymer 1979, 20, 367.
52. Liu, L.; Hu, Y.; Song, L.; Nazare, S.; He, S.; Hull, R. J Mater Sci 2007, 42, 4325.
53. Zhou, Z.; Zhang, Y.; Zeng, Z.; Zhang, Y. J Appl Polym Sci 2008, 110, 3745.